



HAL
open science

Mixture experimental design applied to gallium-rich $\text{GaO}_{3/2}\text{-GeO}_2\text{-NaO}_{1/2}$ glasses

Téa Skopak, Patricia Hée, Yannick Ledemi, Marc Dussauze, Scott Kroeker,
Thierry Cardinal, Evelyne Fargin, Younès Messaddeq

► **To cite this version:**

Téa Skopak, Patricia Hée, Yannick Ledemi, Marc Dussauze, Scott Kroeker, et al.. Mixture experimental design applied to gallium-rich $\text{GaO}_{3/2}\text{-GeO}_2\text{-NaO}_{1/2}$ glasses. *Journal of Non-Crystalline Solids*, 2017, 455, pp.83-89. 10.1002/pssc.201600132 . hal-01417699

HAL Id: hal-01417699

<https://hal.science/hal-01417699>

Submitted on 20 Jan 2017

HAL is a multi-disciplinary open access archive for the deposit and dissemination of scientific research documents, whether they are published or not. The documents may come from teaching and research institutions in France or abroad, or from public or private research centers.

L'archive ouverte pluridisciplinaire **HAL**, est destinée au dépôt et à la diffusion de documents scientifiques de niveau recherche, publiés ou non, émanant des établissements d'enseignement et de recherche français ou étrangers, des laboratoires publics ou privés.

Mixture experimental design applied to gallium-rich $\text{GaO}_{3/2}\text{-GeO}_2\text{-NaO}_{1/2}$ glasses

Skopak T., Hee P., Ledemi Y., Dussauze M., Kroeber S., Cardinal T., Fargin E., Messaddeq Y.

Affiliation: *Notice hal-01417699*

Abstract :

A mixture-design method was used as a multivariate data analysis tool to investigate properties of gallate glasses in the $\text{GaO}_{3/2}\text{-GeO}_2\text{-NaO}_{1/2}$ system. The objective was to design compositions having gallium oxide as the main component of the glass expected for further applications like wave guided transmission in the near- and mid-infrared optical domain. Accordingly to this tool a set of glass compositions were defined in a constrained domain of the ternary glass system rich in gallium oxide and prepared by the traditional melt-quenching technique. Sample density, refractive index, multiphonon cut-off wavelength as well as thermal characteristics were measured as representative multiple responses and a linear model fitting those physical properties vs glass composition was established. The obtained model allows to predict and optimize the different responses for any composition in the studied domain and a better understanding of the influence of each glass component on its physical properties. This study demonstrates that gallium-richest compositions lead to an increase in the polarizability and contribute to a slight enlargement of the transmission window which are the primary conditions requested for intended applications. Complementary structural investigation allows to confirm the influence of the component content in the glass composition revealed by the model.

1. Introduction

The demand for adapted glass compositions implemented in optical applications is continuously rising in the near and mid-infrared (up to 5 μm) where most of the molecules present a fingerprint absorption (harmonic vibrations). Silicate, phosphate and aluminate glasses have been widely investigated for NIR applications [1] but little attention has been devoted to gallate glass matrices, which are potentially excellent candidates. Some studies on binary and ternary gallium oxide containing glasses have been reported in the literature [2], [3], [4], [5], [6], [7], [8], [9], [10], [11], [12], [13] and [14] but only a few present a gallium oxide rich content.

From a structural point of view, gallium is expected to act like aluminum in the vitreous oxide network. When the latter is introduced to an alkali-silica glass system, Si^{4+} ions can be substituted by Al^{3+} ions, which are then compensated by alkali ions, thus reducing the number of non-bridging oxygens (NBOs) [15] and [16]. Regarding optical properties, gallate glasses are expected to exhibit a wider transparency window in the middle infrared compared to classical oxide glasses [10], [17], [18] and [15], such as borates, phosphates or silicates, because of the higher atomic weight of gallium. Also they exhibit significant polarizability and hyperpolarizability which makes them promising materials for nonlinear optical properties [17]. Their low phonon energy ($\sim 850 \text{ cm}^{-1}$ for germanogallate glasses, $\sim 675 \text{ cm}^{-1}$ for some alkali-earth-gallate glasses [13] and [19]) makes them of interest for hosting rare-earth ions in luminescent and laser materials [20]. From the foregoing gallate-based glasses would offer an excellent compromise for mid-infrared transmission applications with the required thermal stability and mechanical resistance for fiber waveguide shaping [21]. Recently, studies on optical waveguiding with gallophosphate glasses have been reported by Vangheluwe et al. [22] but none with compositions rich in gallium oxide. Most of the previous investigations conducted on germanogallate glass systems, which are expected to fulfill these properties, have been focused on the germanium oxide (GeO_2) rich portion of the glass system [5], [8], [10], [18], [20], [23], [24], [25], [26], [27], [28] and [29].

On the contrary this study will focus on the investigation of gallium-rich glass compositions belonging to the sodo-germanogallate ternary system with the perspective of applications in the mid-infrared range (3 to 5 μm). For this purpose, a first modelling of the glass properties (thermal stability toward crystallization, IR transmission, linear refractive indices and density) is explored with the mixture design technique in the gallium oxide rich system. In our knowledge, this represent the first study in the literature with this system which does not permit an effective use of properties calculations features from a glass property database as the SciGlass information system [30]. Properties linear modelling of the measured properties is expected to predict the influence of each component in the studied domain. Complementary structural investigations will be conducted using Raman and ^{71}Ga NMR spectroscopy to confirm, precise and support the model predictions.

2. Experimental details

2.1 Glass preparation

Here, the used components for the ternary composition studied system are $\text{GaO}_{3/2}$, GeO_2 and $\text{NaO}_{1/2}$ which are more relevant to highlight the role of each cation. Glasses in the $\text{GaO}_{3/2}$ - GeO_2 - $\text{NaO}_{1/2}$ system were then prepared by traditional melt-casting technique from gallium oxide Ga_2O_3 (99.99%), germanium oxide GeO_2 (99.99%) and sodium carbonate Na_2CO_3 (99.95%). The weighed and mixed powders were pre-sintered at 950 °C for 1 h and then melted in platinum crucible in ambient atmosphere for 30 min at 1300–1550 °C depending on the compositions. The melted glasses were poured on a stainless steel mold preheated at 40 °C below the glass transition temperature and annealed for 6 h at the same temperature before being slowly cooled to room temperature. All the obtained glasses were colorless, transparent and bubble-free. The glass samples were finally cut and polished on both parallel faces for optical characterization.

2.2 Characterization techniques

2.2.1. Physico-chemical and optical response measurements

Two physico-chemical experimental responses, density and thermal stability, are studied here. The density of the glass, ρ , is related to composition and structural evolution, as well as the thermal stability against crystallization, corresponding to the difference, ΔT , between the onset temperature of crystallization and the glass transition temperature. The latter must be as large as possible (≥ 100 – 120 °C) to facilitate any future technological transfer. Two optical parameters are also studied: the IR cut-off wavelength, which is crucial for mid-infrared applications, and the refractive index, n , which is expected to be the signature of high third-order optical susceptibilities which can be involved in higher level applications like Raman gain or frequency mixing [31] and [32].

Confirmation of nominal glass stoichiometry was verified with a deviation of ± 2 mol% by using Electron Probe Micro Analysis on a VG Microlab 310F apparatus. The glass transition temperature, T_g , and the onset temperature of crystallization, T_x , were determined by differential scanning calorimetric (DSC), using a Netzsch DSC Pegasus 404F3 apparatus on glass pieces in Pt pans at a heating rate of 10 °C/min and with a precision of ± 2 °C. The glass density was determined at room temperature by the Archimedes' method with an Alfa-Mirage MD-300S densimeter using deionized water as immersion liquid. The measurement precision was estimated to be ± 0.01 g/cm³.

The infrared transmission spectra were recorded on glass samples of about 2 mm thickness on a FTIR Perkin Elmer Frontier spectrometer. The linear refractive index was measured by employing the M-lines prism coupling technique (using a Metricon 2010) at 532 nm with an accuracy of ± 0.005 .

2.2.2. Complementary structural characterization

The Raman spectra were obtained using a Horiba Jobin-Yvon LabRAM HR800 micro-Raman spectrometer equipped with a 532 nm laser.

^{71}Ga magic-angle spinning NMR spectra were recorded in a magnetic field of 21.1 T using a Bruker Avance II 900 MHz spectrometer at the Canadian National Ultrahigh-field NMR Facility for Solids (Ottawa, Ontario). Samples were ground to a fine powder, packed into 1.3 mm (outer diameter) rotors and spun at 60 kHz. Single-pulse excitation with a 15 degree tip angle was used to acquire 8000 transients, separated by an optimized relaxation delay of 5 s. The chemical shift reference was 1 M $\text{Ga}_2(\text{SO}_4)_3$ (aq) at 0 ppm. Spectra were fit using a Cjzek model in the software package dmfit [33], which allows parameter distributions suitable for network-forming oxide glasses [34].

3. Design of experiments: glass composition study in the $\text{GaO}_{3/2}\text{-GeO}_2\text{-NaO}_{1/2}$ system

3.1. Definition of the experimental domain

The realization of an optimized design of experiments provides a maximum of information with a minimum of experiments. Within the context of the selection of compositions belonging to the ternary $\text{GaO}_{3/2}\text{-GeO}_2\text{-NaO}_{1/2}$ system, designing experiments consists in polynomial modelling of the properties of interest defined in terms of responses of the system as a function of the composition. Here, the cationic molar percentages of $\text{GaO}_{3/2}$, GeO_2 and $\text{NaO}_{1/2}$ are noted x_{Ga} ; x_{Ge} ; x_{Na} respectively.

In a first step, a preliminary exploratory experiment was performed using the selected preparation method to reach a first piece of information and permit the definition of the domain of study. In this case, the central point in the ternary diagram (domain of compositions) where $x_{\text{Ga}} = x_{\text{Ge}} = x_{\text{Na}} = 33.3\%$ was prepared and characterized (composition N°2 in Fig. 1, Table 1 and Table 2). In order to define our experimental domain, the range of variations of the x_{Ga} , x_{Ge} and x_{Na} compositions and the relational constraints between variables were fixed [35]. The sum of x_{Ga} , x_{Ge} and x_{Na} , *i.e.* of all the oxides percentages, must equal to 100%. The gallium oxide $\text{GaO}_{3/2}$ content was selected to be larger than that of germanium oxide GeO_2 , to focus on rich-gallate glasses and investigate the role played by the gallium cation as a main constituent of the glass network. This leads to the following constraints equations:

$$x_{\text{Ga}} + x_{\text{Ge}} + x_{\text{Na}} = 100 \text{ mol\%}$$

$$x_{\text{Ga}} \geq x_{\text{Ge}}$$

The range of variation for each parameter x_{Ga} , x_{Ge} and x_{Na} was fixed around 10 mol% to stay in the homogeneous glass-forming region and to build up a linear model of the experimental responses:

$$\text{GaO}_{3/2}(\text{mol\%}) : 33 \leq x_{\text{Ga}} \leq 44$$

$$\text{GeO}_2(\text{mol\%}) : 24 \leq x_{\text{Ge}} \leq 34$$

$$\text{NaO}_{1/2}(\text{mol\%}) : 29 \leq x_{\text{Na}} \leq 38$$

These ranges of variations were chosen so as to inscribe the domain of study inside a reduced equilateral triangle moved from the central preliminary test to the richest part of gallium oxide in the ternary diagram. The reduced triangle and domain of composition are depicted in the diagram presented in Fig. 1.

3.2. Determination and quality of the design of experiments

The optimal design of glass compositions was obtained by using the ‘optimal-D’ criterion of optimization from the “Design Expert[®]” version 8 software [36]. Eight experiments, *i.e.* glass compositions, were selected, including the exploratory point. Adjustments were necessary for some compositions which proved to be outside the glass-forming region after preparation, using the conditions described above. In order to construct the model, compositions rich in information and showing glass-forming ability were therefore provided by the software. The final compositions are given in Table 1 and are represented in the ternary diagram shown in Fig. 1. Note that we are considering cationic relative concentrations in the present study to facilitate our investigation of the role played by gallium as a main glass constituent.

After measurements of the four selected physico-chemical and optical responses for the eight designed experiments, each response can be predicted in the domain of study by the use of a linear model with respect to wGa , wGe , wNa representing the reduced molar fractions in the reduced ternary diagram shown on Fig. 1, as expressed in Eq. (1)[31].

$$\text{Response} = a \cdot wGa + b \cdot wGe + c \cdot wNa \quad (1)$$

With wGa , wGe , wNa comprised between 0 and 1 and $wGa + wGe + wNa = 1$.

Reduced variables being comprised between 0 and 1 allow further direct comparison between a , b and c coefficients showing the estimated response for each corner of the reduced triangle. For example, if $wGa = 1$ and $wGe = wNa = 0$, for point A of the reduced ternary diagram in the direction of the richest compositions in gallium oxide, then the response is the coefficient a . The model coefficients a , b and c have then comparable values and they are estimated with their uncertainty depending on the remaining degrees of freedom for a confidence factor of 95%, considering a normal distribution of the response measurement [31]. The coefficient's estimated values give directly the possibility to evaluate the relative weights of the compositions on the studied response. They can be considered to be significant if the relative uncertainties for all estimations remain below 10%. The variance inflation factors are calculated in order to quantify the severity of multicollinearity in the least squares regression analysis leading to the coefficient's estimations [31]. For a good quality regression, these factors would not exceed 5 [31].

4. Results

4.1. Physico-chemical characterization

The measured glass transition temperature T_g , the onset temperature of crystallization T_x , the difference between T_x and T_g ($\Delta T = T_x - T_g$) and the density ρ , are listed in Table 2. The thermal stability against crystallization corresponding to a large ΔT is considered as an important parameter for various practical applications [20]. The multiphonon absorption edge λ_{IR} , calculated here for a linear absorption coefficient of 10 cm^{-1} , as well as the refractive index n (measured at 532 nm), are presented in Table 2.

4.2. Modelling of physico-chemical properties

The coefficients a , b , and c , calculated by the software, for the density ρ , the thermal stability ΔT , the multiphonon cut-off wavelength λ_{IR} and the refractive index n are presented in Table 3 with their respective uncertainties and variance inflation factors. The coefficients, determined for the refractive index, the cut-off wavelength and the density, show excellent agreement with the experimental data (uncertainty below 1%). On the contrary, the coefficients estimated for the thermal stability (uncertainty higher than 12%) can be considered as less significant. All the inflation factors remain below 5, ensuring independent calculations of the coefficients estimations. Those reliable estimated values show equivalent weight of the three oxides normalized relative concentrations on the studied responses.

To predict the glass properties directly on the ternary diagram of composition the four linear models deduced from estimations in Table 3 are used coming back to the linear model given in Eq. (2) with real compositions xGa , xGe and xNa .

$$\text{Response} = a' \cdot xGa + b' \cdot xGe + c' \cdot xNa \quad (2)$$

The dependence of the properties on the components can be mapped by contour line in Fig. 2. In all cases, in the gallium-rich compositions the density and the refractive index increase and the transmission window in the mid-infrared enlarges. For the density, the sodium oxide concentration is clearly unfavorable, the higher density requiring the lower

NaO_{1/2} content as shown in Fig. 2(a). One can observe for a high xGa/xGe ratio the highest density indicating that the gallium-rich compositions have a more compact glass network.

Regarding the refractive index, one can clearly observe in Fig. 2(b) that the polarizability increase is mainly driven by the gallium oxide content, which is in agreement with the data collected by Murthy et al. [14]. Those observations are in accordance with a larger polarizability of the gallium oxide as compared to the germanium oxide [37] and [38]. The increase of gallium oxide, to the detriment of germanium oxide content is the most important parameter for expanding the IR window (Fig. 2(c)). One can observe that the increase of gallium oxide tends to decrease the ΔT as shown in Fig. 2(d).

Then except for thermal properties, the ratio of gallium oxide appears to be the factor with the most important weight in the increase of density and optical properties. Nevertheless the ratio of germanium oxide and sodium oxide play a less important and different role when comparing the density and refractive indices on one side and the cut-off wavelength on another side. Complementary structural characterizations are expected to bring information to explain this interesting observation deduced from the mixture-design model.

4.3. Complementary structural characterizations

The Raman spectra recorded on four glass compositions with various xNa/xGa ratios and chosen for location on different edges of the experimental domain of study (= 1 for N°4: Ga₃₈Ge₂₅Na₃₇ and N°2: Ga₃₃Ge₂₃Na₃₃; and = 0.71 for N°3: Ga₄₂Ge₂₈Na₃₀) are presented in Fig. 3.

The Raman bands are assigned according to McKeown et al. [39]. The band at 300 cm⁻¹ is related to network-modifying cation vibrations in large interstitial sites. The principal band at about 500–550 cm⁻¹ is attributed to vibrations of X—O—X (X = Ga or Ge) bonds. These bonds are in a polymerized network built with GeO₄ and GaO₄ tetrahedra, which are essentially located in rings made of 5 or 6 tetrahedra. The last two bands located at about 750 cm⁻¹ and 870 cm⁻¹ are respectively attributed to GeO₄ and GaO₄ tetrahedra with two non-bridging bonds (chain-like Q² units) and with one non-bridging bond (sheet-like Q³ units). One can note that both bands are slightly shifted toward lower frequencies for N°4: Ga₃₈Ge₂₅Na₃₇.

⁷¹Ga MAS NMR experiments recorded for three selected samples with different xNa/xGa ratios are presented in Fig. 4. A single broad asymmetric peak around 180 ppm is observed for all samples, which is typical for quadrupolar nuclei in glassy environments [40]. The charge-balanced spectra (xNa/xGa = 1) can be modeled using a single site with an isotropic chemical shift of 207 ppm, quadrupole coupling constant of 11 MHz and modest parameter distributions typical of four-coordinate gallium in oxide glasses [41]. With a reduction of sodium content with respect to gallium, additional spectral intensity can be detected on the low-frequency side of the main peak (ca. 100 ppm) which cannot be modeled using a single tetrahedral Ga site, even with more generous parameter distributions. Fig. 4 shows a single-site fit to sample 1, illustrating that additional coordination environments are required to satisfactorily fit the data. Although there is no clear spectral resolution in that region, it may be estimated by difference that approximately 15% of the Ga is found in high-coordinate (5- or 6-fold) sites.

5. Discussion

From the proposed models, it can be deduced that increasing the gallium oxide content produces an increase in density, linear refractive index and multiphonon cut-off wavelength. On the contrary, the thermal stability is reduced with the addition of gallium oxide to the matrix. However, the thermal stability of the prepared glasses remains excellent, *i.e.* larger than 100 °C, over the whole compositional region studied.

The role of the glass network structure on the physical properties has been already investigated from Raman and NMR spectroscopies [39] in the gallium germanate glass system to precise the effects observed from the mixture-design model on these physical properties. The bands observed above 600 cm⁻¹ in the Raman spectra show similar depolymerization of the glass network due to the introduction of sodium oxide content comparable to that of germanium oxide (N°2:

$\text{Ga}_{33}\text{Ge}_{33}\text{Na}_{33}$ compared to N°3: $\text{Ga}_{42}\text{Ge}_{28}\text{Na}_{30}$). For the lowest quantity of germanium oxide and an $x\text{Na}/x\text{Ga}$ ratio around 1 (N°4: $\text{Ga}_{38}\text{Ge}_{25}\text{Na}_{37}$), one can see from Fig. 3 a shift in wavenumber of the band around 870 cm^{-1} attributed to Q^3 units. Henderson et al. [42] have previously attributed in alkali germanate systems the vibration at 835 cm^{-1} to modified Q^3 species. In the $\text{Na}_2\text{O}-\text{GeO}_2$ system such a shift appears for the ratio $x\text{Na}/x\text{Ge} > 1$. This was attributed to the formation of sodium digermanate-like structures. In our case it would correspond to sodium ions acting only as modifiers for the germanium. Such a hypothesis requires a compensation mechanism such as interconnected (mixed corner/edge) gallium oxide entities.

The ^{71}Ga NMR spectra indicate that nearly all of the gallium in these glasses is present in anionic four-fold coordination, as expected to balance the sodium cationic charge. Only when there is insufficient sodium to balance these tetrahedral gallium units is there spectral evidence for high-coordinated gallium. From these observations, the gallium environment can be tentatively described. When $x\text{Na}/x\text{Ga} = 1$, for $x\text{Ge} \leq x\text{Ga}$, each gallium ion occupies an anionic tetrahedral site, the charge being essentially balanced by one sodium cation as there is the same amount of gallium and sodium ions. In such a configuration, the role played by NBOs to compensate the charge of Na^+ cations is negligible. This insertion mode reaches its limit when $x\text{Ga} = x\text{Ge} = x\text{Na}$ (glass composition N°2: $\text{Ga}_{33}\text{Ge}_{33}\text{Na}_{33}$). Indeed, whereas the Na^+ cation charge is already compensated in the vitreous network, additional incorporation of gallium oxide substituted to germanium oxide would preferentially result in the formation of gallium cations with higher (5 or 6) coordination numbers, necessitating new connections between the rings made of GeO_4 and GaO_4 tetrahedra [39]. The formation of such 5 or 6-fold gallium ions can be directly related to the so-called gallate glass, with $x\text{Ga} > x\text{Ge}$ and $x\text{Ga} > x\text{Na}$ (as for glass composition N°1: $\text{Ga}_{44}\text{Ge}_{35}\text{Na}_{31}$). The shoulder observed in the NMR spectra attributed to high coordinated sites in Fig. 4 is effectively observed for the glass composition N°1: $\text{Ga}_{44}\text{Ge}_{35}\text{Na}_{31}$. The addition of high coordinated gallium ions interconnecting the glass network is expected to favor an increase of the density and consequently the refractive index [18]. A more comprehensive NMR characterization will be necessary to prove the existence of high coordinated gallium ions for different compositions where $x\text{Na}/x\text{Ga} < 1$ and to accurately characterize the evolution of the glass-network connectivity vs the cationic ratio $x\text{Na}/x\text{Ga}$. On the contrary the introduction of excess sodium oxide substituted to the germanium oxide from the central point N°2 is expected to break connections in the network leading to new Q^3 species, as observed in the Raman spectra in Fig. 3. The transformation is expected when $x\text{Ga} = x\text{Na}$ for the glass N°4 ($\text{Ga}_{38}\text{Ge}_{25}\text{Na}_{37}$), for which a shift to lower energy of the vibrational bands is observed. For this composition, no shoulder attributed to high coordinated sites can be seen in the NMR spectra, as shown in Fig. 4.

In the studied compositions the formation of a gallate network with the formation of high-coordinated sites due to an increase of $\text{GaO}_{3/2}$ content with a decrease of the ratio $x\text{Na}/x\text{Ga}$ can explain the direction toward high refractive index and density expected from the model (Fig. 2). Regarding the infrared cut-off, Fig. 2 indicates that the polymerization is not a significant parameter, the main parameter remains the lowering of the $x\text{Ge}/x\text{Na}$ ratio. The evolution of the multiphonon cut-off wavelength observed from the model could be related to the shift to lower energy of the vibrational bands (Fig. 3) and the appearance of a new Q^3 unit. One must be cautious in drawing definitive conclusions since the multiphonon edge can correspond to diverse intrinsic vibration combinations.

6. Conclusion

A mixture experimental design, using the optimal-D based design from the “Design Expert®” software, was implemented on glasses from the $\text{GaO}_{3/2}-\text{GeO}_2-\text{NaO}_{1/2}$ ternary system in order to map the evolution of physical properties (thermal stability and density) and optical properties (refractive index and multiphonon cut-off wavelength). A linear model relating each property with the glass composition has been established and represented in a contour line. Correlation using Raman and NMR spectroscopies indicates that replacing germanium oxide by gallium oxide tends to improve the network polymerization through the creation of bridging $\text{Ge}-\text{O}-\text{Ga}$ bonds and probably leads to the insertion into the network of high coordinated gallium ions. The increase in network connectivity results in an increase of the density and the refractive index while maintaining a good thermal stability against crystallization. The multiphonon cut-off wavelength also increases with the $x\text{Ga}/x\text{Ge}$ ratio but for comparable gallium and sodium contents.

Acknowledgements

This research was supported by the Canadian Excellence Research Chair program (CERC) in Photonics Innovations and the Aquitaine Region. The authors are also grateful to the Fonds de Recherche Québécois sur la Nature et les Technologies (FRQNT) (097991) and the Canadian Foundation for Innovation (CFI) (29191 and 32532) for the financial support. Access to the 21.1 T NMR spectrometer was provided by the National Ultrahigh-Field NMR Facility for Solids (Ottawa, Canada), a national research facility funded by a consortium of Canadian universities, supported by the National Research Council of Canada and Bruker Biospin, and managed by the University of Ottawa. We are grateful to Dr Victor Terskikh, Dr. John Wren and Mr. Kirill Levin for valuable assistance with the NMR experiments. Mobilities were supported by grants of the association of Campus France and Mitacs Globalink as well as grants of the Agence Nationale de la Recherche (ANR) with the program "Investissement d'avenir" number ANR-10-IDEX-03-02.

References

1. K.V. Shah, V. Sudarsan, M. Goswami, A. Sarkar, S. Manikandan, R. Kumar, B.I. Sharma, V.K. Shrikhande, G.P. Kothiyal. Preparation and studies of some thermal, mechanical and optical properties of $x\text{Al}_2\text{O}_3(1-x)\text{NaPO}_3$ glass system. *Bull. Mater. Sci.*, 26 (7) (2003), pp. 715–720.
2. J.C. Lapp, W.H. Dumbaugh. Gallium oxide glasses. *Key Eng. Mater.*, 94–95 (1994), pp. 257–278.
3. T. Nishida, H. Ide, Y. Takashima. A linear relationship between the glass transition temperature and local distortion of calcium gallate barium gallate and calcium alluminate glasses. *Bull. Chem. Soc. Jpn.*, 63 (1990), pp. 548–553.
4. A.C. Hannon, J.M. Parker, B. Vessal. The effect of composition in lead gallate glasses: a structural study. *J. Non-Cryst. Solids*, 196 (1996), pp. 187–192.
5. W.H. Dumbaugh, J.C. Lapp. Heavy-metal oxide glasses. *J. Am. Ceram. Soc.*, 75 (9) (1992), pp. 2315–2326.
6. L.G. Hwa, J.G. Shiau, S.P. Szu. Polarized Raman scattering in lanthanum gallogermanate glasses. *J. Non-Cryst. Solids*, 249 (1) (1999), pp. 55–61.
7. D. Ilieva, V. Dimitrov, Y. Dimitriev, G. Bogachev, V. Krastev. Structural study on $\text{Ga}_2\text{O}_3\text{-TeO}_2$ glasses. *Phys. Rev. B*, 39 (4) (1998), pp. 241–245.
8. J. Jewell, P. Higby, I. Aggarwal. Properties of $\text{BaO-R}_2\text{O}_3\text{-Ga}_2\text{O}_3\text{-GeO}_2$ ($R = \text{Y, Al, La, and Gd}$) glasses. *J. Am. Ceram. Soc.*, 77 (3) (1994), pp. 697–700.
9. J. Schwarz, K. Vosejpková. Thermal properties of $\text{Ga}_2\text{O}_3\text{-PbO-P}_2\text{O}_5$ glass system. *J. Therm. Anal. Calorim.*, 104 (3) (2011), pp. 1051–1054.
10. S.S. Bayya, B.B. Harbison, J.S. Sanghera, I.D. Aggarwal. $\text{BaO-Ga}_2\text{O}_3\text{-GeO}_2$ glasses with enhanced properties. *J. Non-Cryst. Solids*, 212 (1997), pp. 198–207.
11. F. Miyaji, T. Yoko, J. Jin, S. Sakka. Neutron and X-ray diffraction studies of $\text{PbO-Ga}_2\text{O}_3$ and $\text{Bi}_2\text{O}_3\text{-Ga}_2\text{O}_3$ glasses. *J. Non-Cryst. Solids*, 175 (1994), pp. 211–223.
12. F. Miyaji, K. Tadanaga, T. Yoko, S. Sakka. Coordination of Ga^{3+} ions in $\text{PbO-Ga}_2\text{O}_3$ glasses as determined by ^{71}Ga NMR. *J. Non-Cryst. Solids*, 139 (1992), pp. 268–270.
13. S. Sakka, H. Kozuka, K. Fukumi, F. Miyaji. Structures of gallate, aluminate and titanate glasses. *J. Non-Cryst. Solids*, 123 (1–3) (1990), pp. 176–181.
14. M.K. Murthy, K. Emery. Properties and structure of glasses in the system $\text{M}_2\text{O-Ga}_2\text{O}_3\text{-GeO}_2$ ($M = \text{Li, Na, K}$). *Phys. Chem. Glasses*, 8 (1967), pp. 26–29.
15. E. Angot, R. Le Parc, C. Levelut, M. Beaurain, P. Armand, O. Cambon, J. Haines. A high-temperature Raman scattering study of the phase transitions in GaPO_4 and in the $\text{AlPO}_4\text{-GaPO}_4$ system. *J. Phys. Condens. Matter*, 18 (17) (2006), pp. 4315–4327.
16. J. Barton, C. Guillemet. *Le verre: Science et Technologie*. EDP Science (2005).
17. J.C. Lapp, W.H. Dumbaugh. Gallium oxide glasses. *Key Eng. Mater.*, 95 (1994), pp. 257–278.
18. P.L. Higby, I.D. Aggarwal. Properties of barium gallium germanate glasses. *J. Non-Cryst. Solids*, 163 (3) (1993), pp. 303–308.
19. K. Fukumi, S. Sakka. Raman spectroscopic study of the structural role of alkaline earth ions in alkaline earth gallate glasses. *J. Non-Cryst. Solids*, 94 (1987), pp. 251–260.
20. X. Wen, G. Tang, J. Wang, X. Chen, Q. Qian, Z. Yang. Tm^{3+} doped barium gallo-germanate glass single-mode fibers for 2.0 μm laser. *Opt. Express*, 23 (6) (2015), p. 7722.
21. H. Fan, L. Hu, K. Yang, Y. Fang. Structure and physical properties of $\text{Bi}_2\text{O}_3\text{-B}_2\text{O}_3\text{-Ga}_2\text{O}_3$ glasses. *J. Non-Cryst. Solids*, 356 (35–36) (2010), pp. 1814–1818.
22. M. Vangheluwe, F. Liang, Y. Petit, P. Hée, Y. Ledemi, S. Thomas, E. Fargin, T. Cardinal, Y. Messaddeq, L. Canioni, R. Vallée. Enhancement of nanograting formation assisted by silver ions in a sodium gallophosphate glass. *Opt. Lett.*, 39 (19) (2014), pp. 5491–5494.
23. J.M. Jewell, L.E. Busse, K. Crahan, B.B. Harbison, I.D. Aggarwal. Optical properties of $\text{BaO-Ga}_2\text{O}_3\text{-GeO}_2$ glasses for fiber and bulk optical applications. *SPIE*, 2287 (1994), pp. 154–163.
24. Y. Zhao, D. Shi. Effect of alkali metal oxides R_2O ($R = \text{Na, K}$) on 1.53 μm luminescence of Er^{3+} -doped $\text{Ga}_2\text{O}_3\text{-GeO}_2$ glasses for optical amplification. *J. Rare Earths*, 31 (9) (2013), pp. 857–863.
25. B.V. Padlyak, B. Kuklinski. Nature of intrinsic luminescence in the glasses of $\text{CaO-Ga}_2\text{O}_3\text{-GeO}_2$ system. *Radiat. Meas.*, 38 (2004), pp. 593–597.
26. B. Padlyak, O. Vlokh, K. Fabisiak, K. Sagoo, B. Kuklinski. Optical spectroscopy of the Er-doped glasses with $3\text{CaO-Ga}_2\text{O}_3\text{-3GeO}_2$ composition. *Opt. Mater.*, 28 (2006), pp. 157–161.
27. I.A. Bufetov, E.M. Dianov. Bi-doped fiber lasers. *Laser Phys. Lett.*, 6 (7) (2009), pp. 487–504.
28. G. Cao, F. Lin, H. Hu, F. Gan. A new fluorogermanate glass. *J. Non-Cryst. Solids*, 326–327 (2003), pp. 170–176.

29. J. Fan, B. Tang, D. Wu, Y. Fan, R. Li, J. Li, D. Chen, L. Calveza, X. Zhang, L. Zhang. Dependence of fluorescence properties on substitution of BaF₂ for BaO in barium gallo-germanate glass. *J. Non-Cryst. Solids*, 357 (3) (2011), pp. 1106–1109.
30. ITC Inc. SciGlass Professional Version 7.12. (2014).
31. C. Rivero, K. Richardson, R. Stegeman, G. Stegeman, T. Cardinal, E. Fargin, M. Couzi, V. Rodriguez. Quantifying Raman gain coefficients in tellurite glasses. *J. Non-Cryst. Solids*, 345–346 (2004), pp. 396–401.
32. N.L. Boling, A.J. Glass, A. Owyong. Empirical relationships for predicting nonlinear refractive index changes in optical solids. *IEEE J. Quantum Electron.*, QE-14 (8) (1978), pp. 601–608.
33. D. Massiot, F. Fayon, M. Capron, I. King, S. Le Calvé, B. Alonso, J.O. Durand, B. Bujoli, Z. Gan, G. Hoatson. Modelling one- and two-dimensional solid-state NMR spectra. *Magn. Reson. Chem.*, 40 (2002), pp. 70–76.
34. J.B. D'Espinose de Lacaillerie, C. Fretigny, D. Massiot. MAS NMR spectra of quadrupolar nuclei in disordered solids: the Czjzek model. *J. Magn. Reson.*, 192 (2008), pp. 244–251.
35. B. Fleury, N. Godon, A. Ayral, D. Perret, J.-L. Dussossoy, S. Gin. Development of an experimental design to investigate the effects of R7T7 glass composition on the residual rate of alteration. *Procedia Mater. Sci.*, 7 (2014), pp. 193–201.
36. J. Goupy. *Plans d'expériences: les mélanges*, Dunod. (2001).
37. H. He, R. Orlando, M. Blanco, R. Pandey, E. Amzallag, I. Baraille, M. Rérat. First-principles study of the structural, electronic, and optical properties of Ga₂O₃ in its monoclinic and hexagonal phases. *Phys. Rev. B*, 74 (19) (2006), pp. 1–8.
38. M.J. Weber. *Handbook of Optical Materials*. (2002).
39. D.A. Mckeown, C.I. Merzbacher. Raman spectroscopic studies of BaO-Ga₂O₃-GeO₂ glasses. *J. Non-Cryst. Solids*, 183 (1995), pp. 61–72.
40. S. Kroeker. NMR spectroscopy of glasses. M. Affatigato (Ed.), *Modern Glass Characterization*, Wiley (2015).
41. D. Massiot, T. Vosegaard, N. Magneron, D. Trumeau, V. Montouillout, P. Berthet, T. Loiseau, B. Bujoli. ⁷¹Ga NMR of reference Ga IV, Ga V, and Ga VI compounds by MAS and QPASS, extension of gallium/aluminum NMR parameter correlation. *Solid State Nucl. Magn. Reson.*, 15 (1999), pp. 159–169.
42. G.S. Henderson, L.G. Soltay, H.M. Wang. Q speciation in alkali germanate glasses. *J. Non-Cryst. Solids*, 356 (44–49) (2010), pp. 2480–2485.

Table 1

Theoretical glass compositions utilized for the mixture design (cationic mol%), with their respective number and label ($\text{Ga}_{x'}\text{Ge}_{x''}\text{Na}_{x'''}\text{Na}$ with x' Ga, x'' Ge, x''' Na the rounded values of $\text{GaO}_{3/2}$, GeO_2 , $\text{NaO}_{1/2}$ mol%) used in the text.

Sample number-label	Theoretical cationic composition (mol%)				
	$\text{GaO}_{3/2}$ (xGa)	GeO_2 (xGe)	$\text{NaO}_{1/2}$ (xNa)	xNa/xGa	xGa/xGe
1- $\text{Ga}_{44}\text{Ge}_{25}\text{Na}_{31}$	43.75	25	31.25	0.71	1.75
2- $\text{Ga}_{33}\text{Ge}_{33}\text{Na}_{33}$	33.33	33.33	33.33	1	1
3- $\text{Ga}_{42}\text{Ge}_{28}\text{Na}_{30}$	41.98	28	30.02	0.72	1.50
4- $\text{Ga}_{38}\text{Ge}_{25}\text{Na}_{37}$	37.5	25	37.5	1	1.50
5- $\text{Ga}_{41}\text{Ge}_{24}\text{Na}_{35}$	41	24	35	0.85	1.71
6- $\text{Ga}_{39}\text{Ge}_{28}\text{Na}_{33}$	38.7	28	33.3	0.86	1.38
7- $\text{Ga}_{37}\text{Ge}_{32}\text{Na}_{31}$	37	32	31	0.84	1.16
8- $\text{Ga}_{37}\text{Ge}_{29}\text{Na}_{34}$	36.8	28.9	34.3	0.93	1.27

Table 2

Glass transition temperature T_g , onset temperature of crystallization T_x , thermal stability ΔT , density ρ , multiphonon cut-off wavelength λ_{IR} and refractive index n of the prepared samples.

Sample number-label	T_g (± 2 °C)	T_x (± 2 °C)	ΔT (± 4 °C)	ρ (± 0.01 g/cm ³)	λ_{IR} (± 0.01 μm)	n_{532} (± 0.005)
1- $\text{Ga}_{44}\text{Ge}_{25}\text{Na}_{31}$	620	740	120	3.93	5.94	1.650
2- $\text{Ga}_{33}\text{Ge}_{33}\text{Na}_{33}$	605	732	127	3.82	5.70	1.653
3- $\text{Ga}_{42}\text{Ge}_{28}\text{Na}_{30}$	635	741	106	3.93	5.90	1.672
4- $\text{Ga}_{38}\text{Ge}_{25}\text{Na}_{37}$	590	710	120	3.79	5.90	1.658
5- $\text{Ga}_{41}\text{Ge}_{24}\text{Na}_{35}$	610	728	118	3.88	5.92	1.671
6- $\text{Ga}_{39}\text{Ge}_{28}\text{Na}_{33}$	610	774	164	3.83	5.92	1.671
7- $\text{Ga}_{37}\text{Ge}_{32}\text{Na}_{31}$	605	750	145	3.88	5.89	1.673
8- $\text{Ga}_{37}\text{Ge}_{29}\text{Na}_{34}$	601	732	131	3.82	5.89	1.655

Table 3

Coefficients a , b and c estimated to model the corresponding glass property (density, thermal stability, multiphonon cut-off wavelength and refractive index) with their respective uncertainty and variance inflation factors, according to the relation (1).

Property		Coefficient estimation	Uncertainty	Variance inflation factor
Density	a	3.950	0.025	1.62
	b	3.870	0.035	1.46
	c	3.720	0.035	1.76
Thermal stability	a	110	11.26	1.50
	b	141	15.08	1.46
	c	128	15.32	1.62
Phonon cut-off edge	a	5.95	0.010	2.10
	b	5.85	0.018	1.69
	c	5.89	0.013	1.63
Refractive index	a	1.690	$5.258 \cdot 10^{-3}$	2.03
	b	1.650	$5.760 \cdot 10^{-3}$	1.35
	c	1.640	$5.930 \cdot 10^{-3}$	2.21

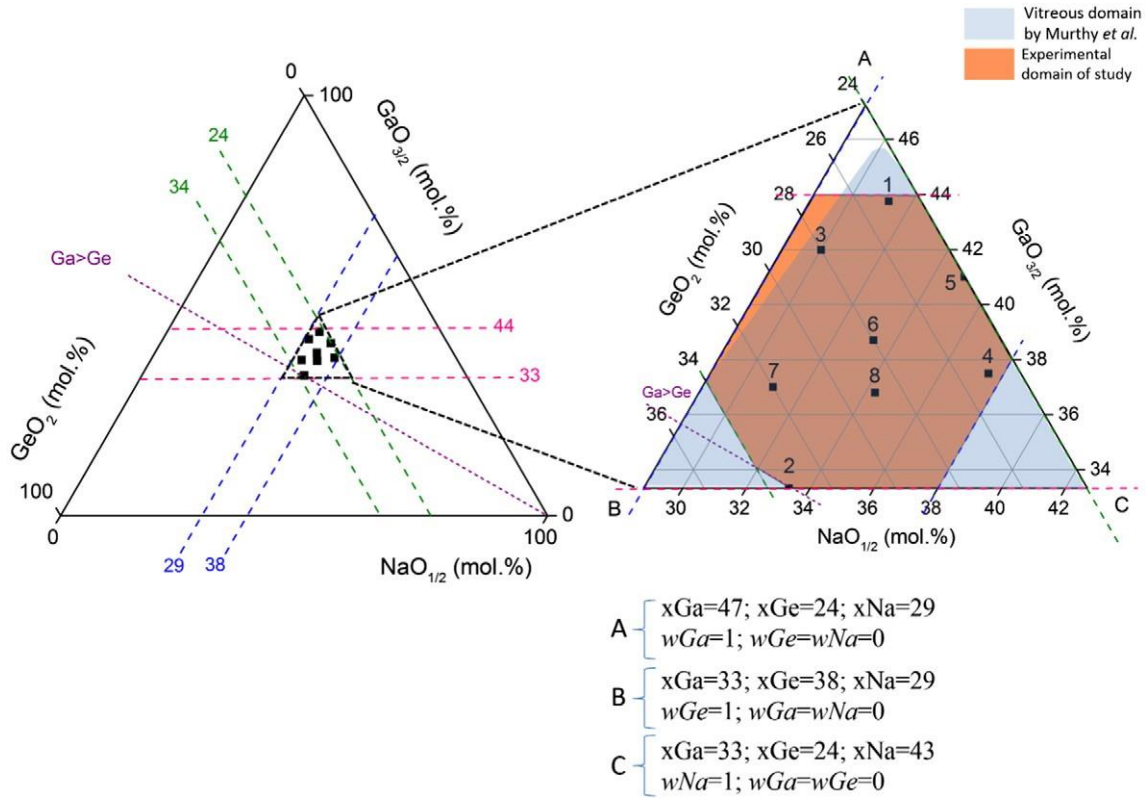


Fig. 1. Ternary $\text{GaO}_{3/2}$ - GeO_2 - $\text{NaO}_{1/2}$ diagram (cationic mol%) representing the determined experimental domain of study (in orange), the vitreous domain determined by Murthy et al. [14] (in blue) and the 8 glass compositions prepared and characterized to build up the model.

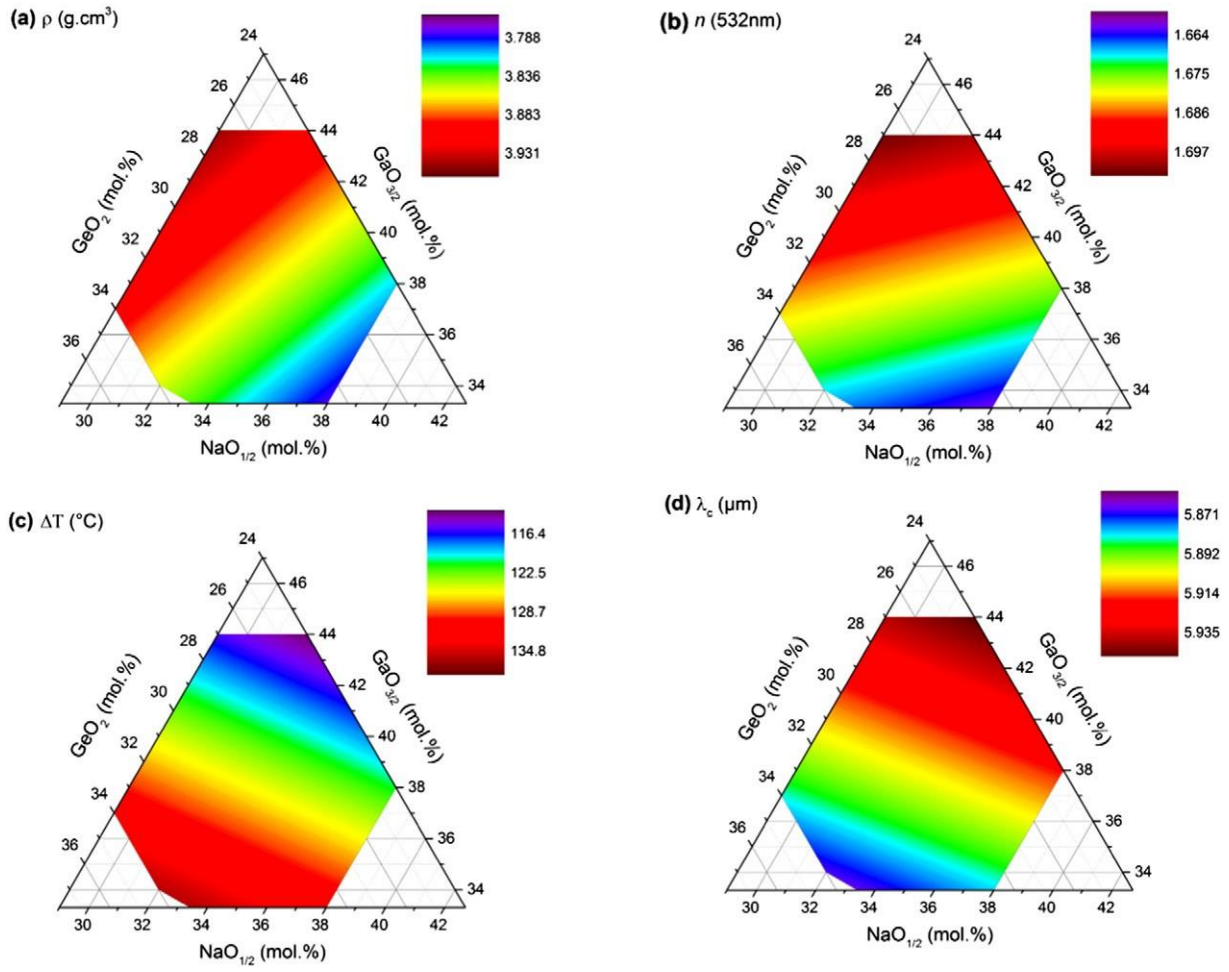


Fig. 2. Contour line representation of the properties in the studied domain. (a) Density, ρ – (b) refractive index, n – (c) thermal stability, ΔT - (d) IR cut-off, λ_c .

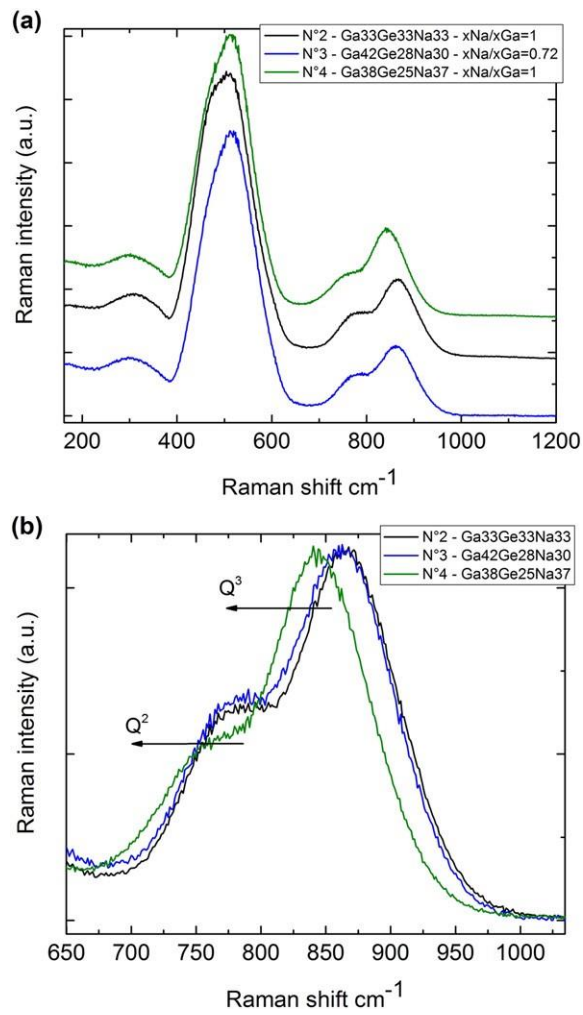


Fig. 3. (a) Raman spectra for GaGeNa glass system with different $x\text{Na}/x\text{Ga}$ ratios – (b) Q3 band normalized Raman spectra for the GaGeNa glass system.

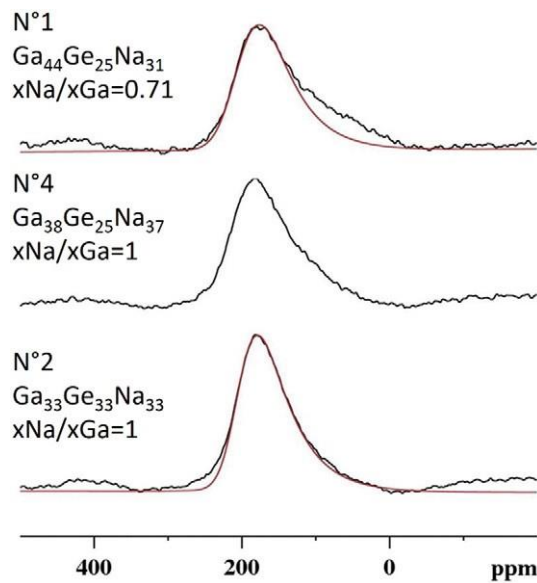


Fig. 4. ^{71}Ga MAS NMR spectra of sodium gallogermanate glasses recorded at 21.1 T with a sample rotation speed of 60 kHz. Red lines represent the best-fit spectrum using a single site (see text).